UCRL--100860

DE90 008541

Contents

DISCLAIMER

Prepared by Yucca Mountain Project (YMP) participants as part of the Civilian Radioactive Waste Management Program. The Yucca Mountain Project is managed by the Waste Management Project Office of the U.S. Department of Energy, Nevada Operations Office. Yucca Mountain Project work is sponsored by the DOE Office of Civilian Radioactive Waste Management.

A DEFORMATION AND THERMODYNAMIC MODEL FOR HYDRIDE PRECIPITATION KINETICS IN SPENT FUEL CLADDING

R. B. Stout
University of California, Lawrence Livermore National Laboratory
P O Box 808, L-200, Livermore, CA 94550

ABSTRACT

Hydrogen is contained in the Zircaloy cladding of spent fuel rods from nuclear reactors. All the spent fuel rods placed in a nuclear waste repository will have a temperature history that decreases toward ambient; and as a result, most all of the hydrogen in the Zircaloy will eventually precipitate as zirconium hydride platelets. A model for the density of hydride platelets is a necessary sub-part for predicting Zircaloy cladding failure rate in a nuclear waste repository. A model is developed to describe statistically the hydride platelet density, and the density function includes the orientation as a physical attribute. The model applies concepts from statistical mechanics to derive probable deformation and thermodynamic functionals for cladding material response that depend explicitly on the hydride platelet density function. From this model, hydride precipitation kinetics depend on a thermodynamic potential for hydride density change and on the inner product of a stress tensor and a tensor measure for the incremental volume change due to hydride platelets. The development of a failure response model for Zircaloy cladding exposed to the expected conditions in a nuclear waste repository is supported by the U.S. DOE Yucca Mountain Project.

INTRODUCTION

Hydrogen in Zircaloy clad spent fuel rods from nuclear reactors can precipitate out as hydride platelets as the temperature decreases during the 10,000 year design life time of a nuclear waste repository proposed at Yucca Mountain, Nevada. The failure of the Zircaloy cladding of a spent fuel rod exposes nuclear waste products to its surroundings. The failure probability for a spent fuel rod due to hydride precipitation depends on the orientation of the hydride platelets [Ostberg, 1968; Einziger and Kohli, 1984]. Typically, fuel rods with low fission gas release have low internal pressures and their hydride platelets precipitate with the normal to the platelet's plane directed radially. In this case, the failure probability due to hydride preciptation is small. However, the precipitation orientation of hydride platelets

depends on the state of stress in the Zircaloy cladding [Ells, 1968; Leger and Donner, 1984]. Thus, for fuel rods with higher fission gas release and higher internal pressures, the probability is increased that the thin hydride platelets will precipitate with their normals in the hoop (tangential) direction of the fuel rod. In this case, the rod's failure probability due to hydrides is greatly increased for two reasons. First, the hydrides are brittle in comparison to Zircaloy, and the hydride platelets with their planes aligned in the radial direction provide a likely crack propagation pathway across the thickness of the cladding. Secondly, the accumulated hoop strain from hydride platelets with their planes aligned in a radial direction increases the potential for surface cracks through the normally protective zirconium oxide film on the cladding. This could result in subsequent cladding failure from stress corrosion cracking.

Because the number of hydride platelets is probablistic, concepts from classical statistical mechanics are used in the following sections to model relative deformation and thermodynamic functionals that depend on a stochastic hydride density function. This hydride density function describes the number of hydride platelets per unit spatial volume per unit species. A hydride platelet species is identified by its physical attributes of size, orientation, and growth rate. A general Boltzmann type balance equation [Boltzmann, 1964] is written to describe the evolution of the hydride platelet density function. In order to quantify terms in this general equation, it is necessary to develop a physical model for both deformations and thermodynamics due to hydride platelets.

Deformations that depend on hydride density are described in terms of a relative deformation functional that has a continuum contribution and discontinuum contribution. The continuum contribution of atomic lattice distortions is represented by continuous functions as in classical continuum mechanics. The discontinuum contribution is represented by an integral type functional that has the hydride platelet density as its function arguments. This functional describes the finite and discontinuous changes in atomic lattice dimensions between zirconium atoms when a zirconium atom is transformed into a zirconium hydride molecule during hydrogen precipitation. From this representation of relative deformation, other kinematic measures that are analytically related to material deformations such as relative velocity, velocity gradients, strains, etc., can be described. All are functionals which depend explicitly on the hydride density function.

The major result of this analysis is a thermodynamic model for stress and deformation dependent kinetics of hydride platelets. The thermodynamic model development applies the classical equilibrium thermodynamic concepts of Gibbs [1961]. The brief discussion of

nonequilibrium thermodynamic processes during hydride precipitation uses the irreversible thermodynamic approach developed initially by Onsager [1931] and described in greater detail by deGroot [1957]. In this short paper, only a brief development is possible. Two useful results of the model are an expression for stress-deformation work influence on the statistical orientation of hydride platelet precipitation and growth, and an expression for the probable strain-deformation field due to hydride platelet precipitation and growth. These expressions were not available from the classical thermodynamic theories of precipitation [Hardy and Heal, 1961; Christian, 1965; Lupis, 1983], partly because the classical theories do not statistically represent the deformation from hydride platelet precipitation and growth. Both of these expressions will be required to plan hydriding experiments and to complete model development for the probable failure rate of hydriding Zircaloy cladding in a prescribed environmental history similar to that expected in a nuclear waste repository.

STATISTICAL DESCRIPTION OF HYDROGEN AND HYDRIDE DENSITIES

During the operation of a nuclear power reactor containing Zircaloy clad fuel rods, hydrogen ingress occurs into the Zircaloy. The hydrogen atoms migrate about as interstitial atoms between zirconium atoms in the Zircaloy matrix and diffuse down hydrogen concentration gradients and down temperature gradients [Sawatzky, 1960]. To develop the subsequent thermodynamic model for hydride platelets, the density of hydrogen atoms moving at velocity $\underline{v}$ relative to the Zircaloy is denoted by a density function $H(\underline{x},t,\underline{v})$. This function is an analog to the one proposed by Boltzmann [1964] to describe gas atoms. In the following analysis a solution for the density function H is fortunately not explicitly required; it is only necessary to have the general concept that species of hydrogen atoms with velocity $\underline{v}$ can be described in terms of a density function (distributed over $\underline{v}$) from which a flux of hydrogen atoms at velocity $\underline{v}$ can be readily expressed as $\underline{v}H$. Finally, the following model will not represent the interatomic displacements that occur as a result of the interstitial hydrogen atoms in the Zircaloy matrix. These interatomic displacements are small in comparison to the discontinuous displacements that occur when dense sets of zirconium and hydrogen atoms locally combine and precipitate as platelets of zirconium hydride. Ideally, the zirconium hydride molecules form and/or dissolve at the solubility limit of hydrogen in the Zircaloy matrix. Upon formation, the hydrides precipitate as thin platelets surrounded by Zircaloy. A given platelet may increase or decrease in size by a flux of hydrogen atoms to or from the platelet boundary. A statistical description of these hydride platelets is the first step in developing a deformation and thermodynamic model for hydride kinetics.

A generic hydride platelet in Zircaloy has dimensional attributes of effective or averaged thickness, area, and orientation. The thickness dimension is much smaller than the two orthogonal dimensions that can be associated with the platelet area. In order to describe different species of hydrides, as well as to subsequently describe discontinuous deformations that result from hydride formation, the thickness of a hydride will be described by the effective number of zirconium hydride molecules, m, times an effective incremental change in the Zircaloy atomic lattice parameter which occurs, as zirconium is transformed into zirconium hydride. Thus, the thickness, $\underline{c}$, which has a vector property because of its directionality relative to the platelet orientation, can be denoted by

$$c_i = m\Delta c_i + mc_{oi} \qquad (1)$$

where m is the effective number of zirconium hydride molecules for a platelet thickness, Δc_i is the incremental dimensional change between zirconium atoms in the lattice structure when the matrix of Zircaloy (zirconium atoms) is transformed to zirconium hydride of the platelet, and c_{oi} is the lattice dimension of the initial Zircaloy atomic lattice structure. The area of a hydride platelet has two attributes, which are denoted by orthogonal vectors $\underline{a}$ and $\underline{b}$ such that their vector cross product gives an effective measure of the area and simultaneously the orientation of the area; i.e. the vector measure of hydride area $\underline{A}$ is

$$A_j = e_{jkl}a_k b_l \qquad (2)$$

where e_{ijk} is the Cartesian alternating tensor, and provides a shorthand notation to write the vector cross product to describe area and orientation of area for a platelet. The magnitudes of vectors $\underline{a}$ and $\underline{b}$ are effective dimensions of the platelet. For example, nearly circular, but yet irregularly shaped platelet areas are effectively represented as circular with a radius multiplied by $(\pi)^{1/2}$; and then the magnitudes of $\underline{a}$ and $\underline{b}$ are equal to give the correct area measure. More elliptically shaped platelet areas would not have equal magnitudes of $\underline{a}$ and $\underline{b}$, but both will be understood to contain the factor $(\pi)^{1/2}$.

The above four physical attributes can be used to identify different hydride platelet species. For cylindrical cladding, radial and tangential (hoop) species of hydride platelets are illustrated in Figure 1. However, if the evolution kinetics of platelets is to be described, then additional rate attributes must be defined. For effective thickness changes, the attribute $\dot{m}$ can be used to denote the time rate of change m. The thickness growth rate attribute describes the change in the effective number of layers of zirconium atoms being transformed into effective layers of zirconium hydride molecules symmetrically on the top (+$\underline{c}$ direction) and bottom (-$\underline{c}$

direction) surfaces simultaneously. Likewise for area and orientation changes, the attributes $\dot{a}_i$ and $\dot{b}_i$ can be used to denote the time rate of change for vectors $\underline{a}$ and $\underline{b}$, respectively. Here, it will also be assumed that the platelets grow symmetrically with respect to their center. The other attribute for hydride platelets was the effective incremental change in lattice dimension, Δc_i, *in the thickness* direction of a platelet which results when zirconium becomes zirconium hydride. For the present model, the magnitude of the vector Δc_i will be assumed to be a constant; this leaves only a possible rotational time-dependence for the vector Δc_i. This rotational time-dependence can also be removed as an attribute for this model of hydride platelet evolution by choosing the vector direction of Δc_i as always aligned and parallel with the platelet normal defined in equation (2). This selection, which also gives the correct volume change due to hydride precipitation and dissolution, means that each platelet has a set of locally dimensioned coordinate vectors, namely ($\underline{a},\underline{b},\Delta\underline{c}$), at its center. Furthermore, the rates $\dot{a}_i$ and $\dot{b}_i$ are independent physical attributes for platelet orientation and area growth.

Thus, for the identification of a generic species, the physical attri-butes are given as a set of variables ($m,\underline{a},\underline{b},\Delta\underline{c},\dot{m},\dot{a}_i,\dot{b}_i$). The probable number density for a species of hydrides at point $\underline{x}$ and time t is denoted by $h(\underline{x},t;m,\underline{a},\underline{b},\Delta\underline{c},\dot{m},\dot{a}_i,\dot{b}_i)$. For shorthand purposes, the set of physical attributes will be represented as a row matrix denoted by $\mathbf{q}$ (i.e., $\mathbf{q}$ = $(m,\underline{a},\underline{b},\Delta\underline{c},\dot{m},\dot{a}_i,\dot{b}_i)$. The domain of all $\mathbf{q}$ values will be denoted by an attribute space Q. The physical meaning of the function $h(\underline{x},t;\mathbf{q})$ is the probable number of hydride platelets at time t in a $d\underline{x}$ volume neighborhood of spatial point $\underline{x}$ and in a $d\mathbf{q}$ species volume neighborhood of point $\mathbf{q}$ in attribute space Q.

The balance equation for the density evolution of a particular species $\mathbf{q}$ of hydride platelet is derived analogously to evolution equations for dislocation density and crack density [Stout, 1981; Stout, 1984], and is

$$\dot{\overset{+}{h}}(\underline{x},t,\mathbf{q}) = \Phi(\underline{x},t,\mathbf{q}) + \int_Q K^+(\underline{x},t,\mathbf{q}^*\rightarrow\mathbf{q})d\mathbf{q}^* - \int_Q K^-(\underline{x},t;\mathbf{q}\rightarrow\mathbf{q}^*)d\mathbf{q}^* \qquad (3)$$

where $\Phi(x,t,\mathbf{q})$ is the net density production of new hydrides for species $\mathbf{q}$, K^+ is the net density increase from all other hydrides species $\mathbf{q}^*$ going into hydride species $\mathbf{q}$, K^- is the net density decrease of hydride species $\mathbf{q}$ going out to all other hydride species $\mathbf{q}^*$, and the total time rate of change for the hydride species density at spatial point $\underline{x}$ is defined as

$$\dot{\overset{+}{h}}(x,t,\mathbf{q}) = \partial_t h(x,t,\mathbf{q}) + \nabla\cdot(\underline{v}h(x,t,\mathbf{q})) \qquad (4)$$

where $\underline{v}$ is the local material velocity of Zircaloy surrounding the hydride relative to a fixed reference set of coordinates. Note that equation (4) for the time rate of change of hydride platelet species **q** at spatial point $\underline{x}$ does not allow for relative motion of the hydride platelets with respect to the surrounding Zircaloy. To allow for the transport of hydride platelets relative to the surrounding Zircaloy would require a refinement on the previous assumption of symmetrical platelet growth described by only two platelet attribute vectors $\dot{a}_i$ and $\dot{b}_i$.

The evolution equation (3) for hydride platelet density is completely general. For applications involving a stress dependence on platelet orientation, analytical forms must be derived for the production and species exchange expressions denoted by Φ, K^+, and K^-, respectively. Physically consistent forms can be derived for these expressions after hydride dependent deformations and thermodynamics are analyzed in the following sections.

RELATIVE DEFORMATION FUNCTIONAL DURING HYDRIDE KINETICS

Consider a material body of contiguous atoms that occupies a spatial domain R_o with an exterior boundary surface denoted by a domain ∂R_o. For a material body $R_o + \partial R_o$ that is Zircaloy, the number of zirconium atoms dominates by several orders of magnitude the number of all other atoms. Using this fact, relative deformation will be described in terms of what displacement events are occurring between any two zirconium atoms, say atoms labeled "N" and "M" in the Zircaloy. These two atoms are arbitrarily separated and can be connected by an arbitrary but finite length line, $L(N \rightarrow M)$, that is contained in domain $R_o + \partial R_o$.

For the case of no hydride kinetics, meaning that no precipitation nor dissolution of hydride platelets is occurring at points between the end points for all sub-divisions of line L, then the relative velocity between atoms N and M is represented as in continuum mechanics by a path integral between points N and M as

$$v_i|(N \rightarrow M,t) = \int_{L(N \rightarrow M)} \partial_j v_i dx_j \qquad (5)$$

where $v_i|(N \rightarrow M,t)$ is the velocity of atom M with respect to atom N at time t and $\partial_j v_i$ is the spatial gradient of the velocity vector of atoms along path $L(N \rightarrow M)$. The velocity of equation (5) measures the relative velocity between atoms that is associated with changes in length of

interatomic bonds; but does not include any discontinuities from dislocations, microcracks, cracks, or hydride phase changes.

The set of hydride-induced lattice discontinuities can be represented along path L by considering their displacement events that can occur on the set of arbitrary sub-divisions along line L(N→M) at time t. The hydride displacement events on the line L(N→M) include the spontaneous appearance or disappearance of a hydride platelet, the increase or decrease in the thickness direction of a hydride platelet, and the area growth of a platelet that intersects the line L(N→M). The lattice dimensional changes from the transitions to or from zirconium hydride occur as a displacement discontinuity between atoms in the lattice structure; and results in a discontinuity in the displacement along the path L(N→M). The net velocity from the set of discontinuities can be represented by integrating over the path L(N→M), which sums the rates and magnitudes of discontinuity events. This is written for the relative velocity in terms of the rate of discontinuous contributions due to hydride kinetics as

$$v_i](N \to M,t) = \int_{L(N\to M)} \int_Q m\,\Delta c\, e_{jk} a_k b_l \dot{\bar{h}}(x,t,q) + m\,\Delta c\, e_{jk} \dot{a}_k b_l h(x,t,q) + m\,\Delta c\, e_{jk} \{\dot{a}_k b_l + a_k \dot{b}_j\} h(x,t,q) dq dx_j \qquad (6)$$

where the $v_i](N\to M)$ represents only the discontinuous contributions in relative velocity between atoms N and M on path L; and these contributions are from three types of events in the integrand:

1. the net probable spontaneous hydride appearance at rate $\dot{\bar{h}}$ on path L,

2. the probable growth in hydride thickness at rate $\dot{m}$ on path L,

3. the probable hydride area growth at rate $e_{jk}(\dot{a}_k b_l + a_k \dot{b}_l)$ along path L.

A physical interpretation of the integration for the three types of events can be provided in terms of concepts from classical statistical mechanics. For example, consider the first term in the integrand of equation (6); this represents the projected area probability of the line segment dx_j intersecting a hydride platelet of area $e_{jk}a_k b_l$ for species q. The resulting projected volume would be $e_{jk}a_k b_l dx_j$, which multiplied by the rate of hydride density change, gives the

probability for the appearance (or for $\dot{\bar{h}}$ negative, the disappearance) of hydride platelets of species **q**. Species **q** has the incremental lattice thickness change of $m\Delta c_i$, which is the displacement discontinuity that occurs between zirconium atoms on opposite sides of a newly created hydride platelet of species **q**. Thus, the first term represents the probability for the appearance of a discontinuity of size $m\Delta c_i$ along the path as $e_{jkl}a_k b_l \dot{\bar{h}}(\underline{x},t,\mathbf{q})d\mathbf{q}dx_j$. Note that if the increment of path dx_j is orthogonal to the area $e_{jkl}a_k b_l$, then, consistent with the thin platelet assumption, the probability of line L(N→M) intersecting this species of platelet is zero. A similar physical interpretation of the second term in the integrand can be analogously provided for the rate of thickness growth of hydride platelets that intersect the line increment dx_j. The last term in the integrand contains the area growth rate of the platelets, and it physically represents the probability for the rate that platelets will grow and intersect line segment dx_j. Each such intersection brings a lattice displacement discontinuity of the hydride platelet species $m\Delta c_i$. The integration over all species **q** in set Q and all increments dx_j on line L(N→M) sum up the rate of displacement discontinuities for the probable relative discontinuum velocity due to hydride kinetics. For future shorthand notational purposes, the integration over the attribute space Q can be defined by integral operators as follows:

$$C_{ij}(\,) \equiv \int_Q m\Delta c_i e_{jk} a_k b_l(\,)\, d\mathbf{q} \qquad (7a)$$

$$\dot{C}_{ij}(\,) \equiv \int_Q \dot{m}\Delta c_i e_{jk} a_k b_l(\,)\, d\mathbf{q} \qquad (7b)$$

$$\dot{A}_{ij}(\,) \equiv \int_Q m\Delta c_i e_{jk} \dot{a}_k b_l(\,)\, d\mathbf{q} \qquad (7c)$$

$$\dot{B}_{ij}(\,) \equiv \int_Q m\Delta c_i e_{jk} a_k \dot{b}_l(\,)\, d\mathbf{q} \qquad (7d)$$

where C_{ij} operates on the function $\dot{\bar{h}}$ and the remaining three operators, $\dot{C}_{ij}$, $\dot{A}_{ij}$ and $\dot{B}_{ij}$, operate on the function h.

The total relative velocity of atom "M" with respect to atom "N" is the sum of the continuous and discontinuous contributions given by equations (5) and (6), respectively, and is denoted as

$$v_i\}(N\rightarrow M,t) = v_i|(N\rightarrow M,t) + v_i\rfloor(N\rightarrow M,t) \qquad (8)$$

where the single brace symbol "}" denotes the total of a quantity, the single bar symbol "|" denotes the continuous contribution of a quantity, and the single square bracket "]" denotes the discontinuous contribution of a quantity. For example, the relative displacement of atom "M" with respect to atom "N" is the time integration of equation (8), which is written as

$$u_i\}(N\rightarrow M,t) = u_i|(N\rightarrow M,t) + u_i\rfloor(N\rightarrow M,t) \qquad (9)$$

where it has been assumed that at time t=0 the initial relative displacement is zero. Then the notation indicates that $\underline{u}\}$ is the total relative displacement of atom M with respect to N at time t, $\underline{u}|$ is the continuous contribution to the relative displacement, and $\underline{u}\rfloor$ is the discontinuous displacement contribution due to hydride kinetics. Physically, it is known that the total relative displacement $\underline{u}\}$ exists as a unique vector quantity, and is also independent of the path selected between atoms N and M. However, the continuous and discontinuous contributions, $\underline{u}|$ and $\underline{u}\rfloor$, are each path-dependent functionals. For the purposes of this development, it is convenient for notational reasons, and not restrictive with respect to results to use only straight line path segments between atoms. This choice means that the Cartesian tensor notation is sufficient and appropriate for representing the tensor quantities that are subsequently introduced.

To complete the representation of hydride induced deformation response, kinematic measures for strain are necessary. For finite or large changes, the development of strain measures can be derived in terms of a relative deformation functional between atoms in a small, but finite sized, neighborhood. The relative deformation functional is given as

$$\chi_i\}(N\rightarrow M,t) = X_i\}(N\rightarrow M,t=0) + u_i|(N\rightarrow M,t) + u_i\rfloor(N\rightarrow M,t) \qquad (10)$$

where the vector $\underline{\chi}\}$ is a position vector from atom "N" to atom "M" at t, $\underline{X}\}$ is the position vector from atom "N" to atom "M" at time t=0 (which includes contributions from hydride platelets that exist at t=0), and $\underline{u}|$ and $\underline{u}\rfloor$ are the continuous and discontinuous parts of relative

displacements that were described previously which occur after t=0. The continuous contribution, $\underline{u}|$, is represented by a continuous function at intermediate points $\underline{x}$ along line L(N→M). Thus, at point $\underline{x}$ relative to point N, $\underline{u}|(N\rightarrow\underline{x},t)$ is a displacement function that depends continuously on spatial point $\underline{x}$ and time t; and therefore it has a differential. The discontinuous contribution, $\underline{u}]$, is represented by the time integration of the functional of equation (6). Using the operator definitions in equation (7), this can be written for atom "N" at position $\underline{\chi}(N,t)$ and atom "M" at position $\underline{\chi}(M,t)$ for t at time in the interval (0,t) as

$$u_i](N\rightarrow M,t)=\int_o^t\int_{\underline{\chi}(N,\tau)}^{\underline{\chi}(M,\tau)}\int_Q C_{ij}\dot{\bar{h}}(\underline{x},\tau,q)+(\dot{C}_{ij}+\dot{A}_{ij}+\dot{B}_{ij})h(\underline{x},\tau,q)dqdx_jd\tau \quad (11)$$

where it is noted that the path L(N→M) between atoms N and M remains a straight line, and the end-points, as well as the line, translates with atoms N and M for times τ in the time interval (0,t). It can be seen from equation (11) that the continuum methodology [Eringen, 1967] for point-wise strain measures can not be obtained from a spatial differential of equation (10) with respect to either the initial configuration positions at time t=0 or the final positions at time t of material points. This is because equation (11) for the functional $\underline{u}]$ has a function dependence for the complete history of positions $\underline{\chi}(N,\tau)$ and $\underline{\chi}(M,\tau)$ throughout the time interval (0,t) and spatial differentiation for Lagrangian or Eulerian strain measures is not possible. However, it is possible and straightforward to obtain a first order approximation for a spatial differential that is consistent with the physical concepts and modelling objectives of developing kinematic measures from the relative deformation functional $\underline{\chi}$]. The approximation can be obtained by replacing the position dependence of atoms "N" and "M" by either those at time t=0 or those at time t; then the order of integration over time and space can be exchanged. Here, only the Eulerian strain measure will be derived by first replacing atom positions $\underline{\chi}(M,\tau)$ and $\underline{\chi}(N,\tau)$ in equation (11) by their positions at time τ=t, namely, $\underline{\chi}(M,t)$ and $\underline{\chi}(N,t)$, respectively. Then, for atoms M and N in a small spatial neighborhood that contains statistically representative dense sets of hydrides, an incremental representation for the spatial integration can be obtained by interchanges in the time and spatial integrations. This leads directly to a spatial differential as a coefficient tensor $\Delta\,\underline{u}]$ for $\Delta\chi_j$] that can be written as

$$\Delta_j u_i]\Delta\chi_j]=\int_o^t\int_Q C_{ij}\dot{\bar{h}}+(\dot{C}_{ij}+\dot{A}_{ij}+\dot{B}_{ij})\,h dqd\tau\Delta x_j \quad (12)$$

where the spatial increment $\Delta\underline{x}$ is

$$\Delta x_j=\chi_j(M,t)-\chi_j(N,t)=\Delta\chi_j] \quad (13)$$

because it is the incremental coordinate separation as well as the relative spatial vector between atoms N and M at time $\tau = t$. Using equation (12), and the differential property of $\underline{\mu}$, equation (10) can be written in incremental form as

$$\Delta X_{i\underline{j}} = (\delta_{ij} - \Delta_j u_{\underline{i}} - \Delta_{\underline{j}} u_{\underline{i}}) \Delta\chi_{\underline{j}} \tag{14}$$

Because of the probabilistic hydride density, the Eulerian strain tensor, $\gamma_{mn\underline{}}$, is defined as the probable value of the metric measure for the change in separation between atoms M and N during the time interval (o,t) relative to the deformed spatial reference at time $\tau = t$, i.e.,

$$\Delta\chi_{i\underline{}}\Delta\chi_{i\underline{}} - \Delta X_{i\underline{}}\Delta X_{i\underline{}} \equiv 2\gamma_{mn\underline{}}\,\Delta\chi_{m\underline{}}\Delta\chi_{n\underline{}} \tag{15}$$

Substituting equation (14) into equation (15) and decomposing the total strain tensor into functionally independent continuum and hydride-induced discontinuum components, it is found that

$$\gamma_{mn\underline{}} = \gamma_{m\underline{n}} + \gamma_{mn\underline{}} \tag{16}$$

such that the continuum and discontinuum Eulerian strain tensor measures are

$$\gamma_{m\underline{n}} = \frac{1}{2}(\Delta_m u_{\underline{n}} + \Delta_n u_{m\underline{}} - \Delta_m u_{\underline{k}}\,\Delta_n u_{\underline{k}}) \tag{17}$$

$$\gamma_{mn\underline{}} = \frac{1}{2}(\Delta_m u_{n\underline{}} + \Delta_n u_{m\underline{}} - \Delta_m u_{k\underline{}}\,\Delta_n u_{k\underline{}} \tag{18}$$

$$- \Delta_m u_{k\underline{}}\Delta_n u_{\underline{k}} - \Delta_m u_{\underline{k}}\,\Delta_n u_{k\underline{}})$$

The last kinematic relationship that is required for the thermodynamic model derived in the following section is between the strain rates and the gradient of velocity. The Eulerian rate for the continuum strain measure is by definition

$$\dot{\gamma}_{m\underline{n}} = \partial_t \gamma_{m\underline{n}} + v_{\underline{j}} \nabla_{\underline{j}} \gamma_{m\underline{n}} \tag{19}$$

The spatial gradient of the velocity vector follows from the equations (5), (6) and (8) as

$$\Delta_{\underline{j}} v_{i\underline{}} = \Delta_{\underline{j}} v_{\underline{i}} + \Delta_{\underline{j}} v_{i\underline{}} \tag{20}$$

As derived elsewhere [Stout, 1989], the strain rate tensor in equation (19) is related to the strain tensor in equation (17) and the velocity gradient in equation (20) as follows

$$\dot{\gamma}_{ij} = \frac{1}{2}(\Delta_i v_j + \Delta_j v_i) - \gamma_{mi}\Delta_j v_m - \gamma_{mj}\Delta_i v_m$$
$$- \gamma_{mi}\Delta_j v_m] - \gamma_{mj}\Delta_i v_m] \quad (21a)$$

$$= (I_{ijmn} - S_{ijmn})\Delta_m v_n - S_{ijmn}\Delta_m v_n] \quad (21b)$$

where
$$I_{ijmn} \equiv \frac{1}{2}(\delta_{im}\delta_{jn} + \delta_{jm}\delta_{in}) \quad (21c)$$

$$S_{ijmn} \equiv \gamma_{mi}\delta_{jn} + \gamma_{mj}\delta_{in} \quad (21d)$$

and δ_{im} is the second order isotropic tensor. From equations (21) it is seen that the continuum strain rate is coupled to the continuum and discontinuum components of the velocity gradient and the continuum strain tensor. Thus, even for small continuum strains, the kinematic consequences of hydride kinetics can be significant in developing and physically interpreting a thermodynamic model for hydrides in Zircaloy. Finally, the deformation and kinematic measures developed in this section are based on statistical modelling concepts. Therefore, the expressions derived provide probable or expected value measures based on a probabilistic density function that is integrated over all species of hydrides represented statistically in a unit spatial volume element in the neighborhood of a spatial point at a given time. Because of the dense sets of hydrides, this statistical approach is the only mathematical way that the physical aspects of hydride-induced deformation response can be represented effectively for the thermodynamic model developed in the following section.

THERMODYNAMIC MODEL FOR HYDRIDE KINETICS

The previous section developed kinematic expressions that describe deformation processes during the precipitation and growth of hydride platelets. This section will develop energetic expressions that describe thermodynamic processes during the precipitation and growth of hydride platelets. The approach for modelling a thermodynamics of hydride platelet kinetics is analogous to that for thermodynamic models developed for the kinetics of dislocations, cracks, and particle-voids [Stout, 1981; Stout, 1984; Stout, 1989]. The approach begins by assuming a functional form for the thermodynamic internal energy. Then, using functional derivatives, surface-volume integral transformations, and the quasi-static form for the first law of thermodynamics, expressions for the energetics of different thermodynamic rate processes are derived.

The functional form for the internal energy ε in an arbitrary volume R_o with exterior boundary ∂R_o is assumed to be

$$\varepsilon(x,t) = \varepsilon(\eta(\underline{x},t),\ \gamma_{mn|}(\underline{x},t),\ h(x,t,q)\ H(\underline{x},t,\underline{y}),\ Z(\underline{x},t),\ \overline{\partial R}(\underline{x},t)) \qquad (22)$$

where η is the entropy function, $\gamma_{mn|}$ is only the continuum component of the total strain measure, h is the hydride platelet density function, H is the hydrogen atomic density function, Z is the dominant zirconium atomic density function in Zircaloy, and $\partial\overline{R}(\underline{x},t)$ is the density of boundary surfaces between hydride platelets and Zircaloy in R_o. The internal energy functional is assumed smoothly continuous with respect to its functional arguments. The first law of thermodynamics is written for a system consisting of a body R_o with exterior boundary ∂R_o as

$$\int_{R_o} \partial_t \varepsilon dV + \int_{\partial R_o} e_i n_i dA = \int_{R_o} f_i v_i] dV + \int_{\partial R_o} \sigma_{ij} v_j] n_i dA + \int_{R_o} \dot{P} dV - \int_{\partial R_o} p_i n_i dA \qquad (23)$$

where $\partial\varepsilon$ is the point-wise rate of internal energy change in R_o, $e_i n_i$ is the energy flux across ∂R_o, $f_i v_i]$ is the work rate done by body forces in R_o, $\sigma_{ij} v_j] n_i$ is the work rate done by traction forces on ∂R_o, $\dot{P}$ is a heat rate added at points in R_o, and $p_i n_i$ is the heat rate transported across ∂R_o. To derive energetic expressions from equation (23), more explicit representations for the internal energy are required and the integrals over the boundary ∂R_o have to be transformed to integrals over the arbitrary spatial volume R_o. Because the functional ε has been assumed smoothly continuous, the energy rate at points R_o can be written as

$$\partial_t \varepsilon = \Delta_\eta \varepsilon_t \eta + \Delta_\gamma \varepsilon \partial_t \gamma_{mn} I + \Delta_h \varepsilon \partial_t h + \Delta_h \varepsilon \partial_t H + \Delta_z \varepsilon \partial_t Z + \Delta_{\overline{\partial R}} \varepsilon \partial_t \overline{\partial R} \qquad (24)$$

where $\Delta_\eta\varepsilon$, $\Delta_\gamma\varepsilon$, $\Delta_h\varepsilon$, $\Delta_H\varepsilon$, $\Delta_Z\varepsilon$, and $\partial_{\overline{\partial R}}\varepsilon$ are functional operators, as well as thermodynamic potentials, for the rate of change of their associated function rates. For example, $\Delta_h\varepsilon$ is a thermodynamic potential for hydride kinetics and $\Delta_H\varepsilon$ is a thermodynamic potential for changes in hydrogen density. Each operator measures a change in internal energy when a corresponding change in their associated function occurs and are analogs to the chemical potentials defined from Gibbs' free energy function in classical thermodynamics [Gibbs 1964; Lupis, 1983]. The flux of internal energy transported across the exterior boundary can be transported at two velocities; one of which is the dominant mass velocity of the Zircaloy and the other is the atomic mass velocity of hydrogen (recall that hydrides were assumed to have the same velocity as the Zircaloy). Therefore, the internal energy flux is represented with functional operators defined by the thermodynamic potentials on the four associated density functions, namely

$$e_{\mathcal{P}}n_i = (\Delta_h \varepsilon h v_i\} + \Delta_H \varepsilon H\ (v_i\} + v_i) + \Delta_Z \varepsilon Z v_i\} + \Delta_{\overline{\partial R}} \varepsilon \overline{\partial R} v_i\})n_i \qquad (25)$$

which states that the energy transported by hydrides and Zircaloy moves at the material deformation velocity $v_i\}$ and the energy transported by hydrogen atoms moves through hydrides and Zircaloy at velocity v_i relative to their velocity $v_i\}$. Furthermore, equation (25) implies that the internal energy of a body can be written in terms of four additive functional operators that operate on their associated density function; more explicitly,

$$\varepsilon = \Delta_h \varepsilon h + \Delta_H \varepsilon H + \Delta_Z \varepsilon Z + \partial_{\overline{\partial R}} \varepsilon \overline{\partial R} \qquad (26)$$

where each functional operator has the same function arguments as those given previously in equation (22). After substituting the internal energy expressions from equations (24) and (25) into the volume and surface integrals on the left side of equation (23), it is seen that transforming the surface integral into a volume integral would result in several simplifications. To make this transformation requires a number of carefully completed analytical steps, a few new energy definitions, and more explicit and detailed representations for the surface energy expression. Part of the analysis complexity arises because the internal energy functional is not necessarily spatially continuous across the interior boundaries between the hydrides and the Zircaloy. This means that during the growth kinetics for hydride precipitates these interior boundaries propagate at a velocity relative to the local material velocity and an analysis similar to that for a "shock front" is required for this propagating internal energy discontinuity. The analog analysis was developed previously for the energetics of dislocation kinetics across shocks [Stout, 1986] and is only briefly presented here. For hydrides, this analysis requires that the thermodynamic potential (Gibbs' chemical potential) per molecule of zirconium hydride be defined. Here, it will be denoted as $\Delta_{\overline{ZH}}\varepsilon$ and it is set equal to the thermodynamic potential for a species of hydride divided by the number of zirconium hydride molecules in the volume of the hydride species; thus for any species **q**,

$$\Delta_{\overline{ZH}}\varepsilon = \Delta_h \varepsilon / (C_* \rho_{\overline{ZH}}) \qquad (27)$$

$$C_* \equiv C_{*ii} = c_i e_{ijk} a_j b_k \qquad (27b)$$

where $\rho_{\overline{ZH}}$ is the molecular number density of zirconium hydride and C_* is the scalar volume of a species **q** hydride platelet.

In addition to defining the above internal energy expression to treat the spatial discontinuity in the internal energy, the surface energy for the boundary between the hydrides and the Zircaloy matrix also has to be explicitly represented. In contrast to a prior analysis of both surface energy and surface strain energy for cracks [Stout, 1984], only the hydride-Zircaloy surface energy will be represented. This surface energy, which is energy per unit area (what Gibbs denoted as the "superficial density" of energy [Gibbs, 1961]), is represented as a vector quantity. Then the contribution to internal energy of surface energy per unit volume from all hydrides in a unit volume is

$$\Delta_{\overline{\partial R}}\varepsilon\overline{\partial R} = 2\int_Q ((\Delta_a\varepsilon e_{ijk}b_jc_k + \Delta_b\varepsilon e_{ijk}c_ja_k)\pi^{1/2} + \Delta_c\varepsilon e_{ijk}a_jb_k)\, h\,(\underline{x},t,q)dq \tag{28a}$$

$$\equiv 2\Delta_{\underline{\alpha}}\, E\, \underline{\alpha}\, h \tag{28b}$$

where $\Delta_a\varepsilon$, $\Delta_b\varepsilon$, and $\Delta_c\varepsilon$ are surface energy densities for hydride surfaces with corresponding normals in the directions of vectors $\underline{a}$, $\underline{b}$, and $\underline{c}$, respectively; and equation (28b) denotes a shorter notation in terms of a vector of operators, $\Delta_\alpha E$, over the Q hydride species domain, and the three directional vectors, ($\underline{a}$,$\underline{b}$,$\underline{c}$) of a hydride. For example, the surface energy operator and $\underline{a}$ vector for the "$\underline{a}$" components are defined from equation (28b) as

$$\Delta_{\alpha_a}E \equiv \int_Q \Delta_a\varepsilon(\,)dq \tag{29a}$$

$$(\alpha_a)_i \equiv e_{ijk}b_jc_k\pi^{1/2} \tag{29b}$$

and similarly for the $\underline{b}$ and $\underline{c}$ components.

Now, from the above discussion on transforming the energy flux surface integral into a volume integral, and using equations (27) and (28), the following expression can be derived for the rate of internal energy change in an arbitrary volume R_o with boundary ∂R_o:

$$\int_{R_o}\partial_t\varepsilon dV + \int_{\partial R_o} e_{ji}\eta_j dA = \int_{R_o}\Delta_\eta\varepsilon\dot{\eta} + \Delta_{\gamma_{mn}}\varepsilon\dot{\gamma}_{mn}$$

$$\Delta_h\varepsilon\dot{\bar{h}} + \Delta_H\varepsilon\dot{\overline{H}} + \Delta_Z\varepsilon\dot{\overline{Z}} + \underline{\nabla}(\Delta_H\varepsilon)\underline{v}H$$

$$+ 2\Delta_\alpha E\underline{\alpha}\dot{\bar{h}} + 2\Delta_\alpha E\underline{\dot{\alpha}}h \tag{30}$$

$$+ 2(\Delta_{\overline{ZH}}\varepsilon\rho_{\overline{ZH}} - \Delta_H\varepsilon H - \Delta_Z\varepsilon Z)\,\dot{\beta}_i\alpha_i h - 2[\Delta_H\varepsilon H v_i]\dot{\alpha}_i h dV$$

where, in order, the integrand terms denote internal energy rates from the change in entropy, the changes in continuum strain, the volume energy rate during hydride precipitation kinetics, the volume energy rate of hydrogen atoms going into hydride precipitation, the volume energy rate of zirconium atoms (essentially Zircaloy) going into hydride precipitation, the energy rate due to the transport of hydrogen atoms in a gradient of its thermodynamic potential, the surface energy rate during hydride precipitation kinetics, the surface energy rate during hydride platelet growth, the volume energy during hydride platelet growth which occurs when zirconium hydride molecules are formed from hydrogen and zirconium atoms as the hydride boundary propagates at velocity $\dot{\beta}_i(\dot{\beta}_i \equiv (\dot{a}_i, \dot{b}_i, \dot{m}\Delta c_i))$ and sweeps out neighboring areas α_i, and finally the possible energy discontinuity as hydrogen atoms move across hydride platelet boundaries and change from hydrogen atoms that are part of a molecule of zirconium to hydrogen atoms that are interstitially positioned in the Zircaloy matrix; the last two terms are results of the "shock front" analysis for a spatial internal energy discontinuity that propagates. The factors of "2" in the surface energy and growth energy terms occur because it was assumed previously that the hydrides have symmetry in the a, b, and c directions and move with the surrounding Zircaloy. Also, in deriving terms in equation (30), no spatial gradient effects in the directions a, b, and c were included. These are higher order effects with respect to the magnitudes of vectors (a,b,c) when compared with the existing terms and would probably be important only when their coefficients, which are various spatial gradients of the thermodynamic potentials, are extremely large.

Various terms in the above integrand on the right side can be combined; however, it is best to first convert the boundary work rate and the boundary heat transport rate expressions in equation (23) to volume integrals. The traction work rate on the surface ∂R_o can be transformed easily to a volume integral, providing the stress tensor is continuous everywhere in R_o; subject to this assumption, it can be written as [Stout, 1981]

$$\int_{\partial R_o} \sigma_{ij} v_j \} n_i dA = \int_{R_o} \Delta_i \sigma_{ij} v_j \} + \sigma_{ij} \Delta_i v_j \} dV \qquad (31)$$

where $\Delta_i \sigma_{ij}$ is the spatial gradient of the stress tensor and $\Delta_i v_j \}$ is the spatial gradient of the velocity vector that is related to the strain rate tensor by equation (21). The heat vector for the heat transport rate across the surface will also be assumed to be continuous everywhere in R_o, thus the boundary term in equation (23) for heat transport becomes

$$\int_{\partial R_o} p_i n_i dA = \int_{R_o} \Delta_i p_i dV \qquad (32)$$

Now, equation (23) can be rewritten by substituting terms from equations (30), (31), and (32); and after some rearranging and simplifying the following form is obtained that must be valid for all deformation processes;

$$\begin{aligned}\int_{R_o} \Delta_\eta \varepsilon \dot{\eta} dV = \int_{R_o} & \dot{P} - \Delta_i p_i + (\sigma_{ij} - (I_{mnij} - S_{mnij})\Delta_{\gamma_{mn}}\varepsilon)\Delta_i v_j \\ & + (\sigma^*_{ij} C_{ij} - (\Delta_h \varepsilon + 2\Delta_{\alpha_i} E\alpha_i - \Delta_H \varepsilon H C_o - \Delta_Z \varepsilon Z C_o))\dot{\bar{h}} - \Delta_j(\Delta_H \varepsilon) v_j H \\ & + (\sigma^*_{ij}(\dot{A}_{ij} + \dot{B}_{ij} + \dot{C}_{ij}) - (\Delta_{\overline{ZH}} \varepsilon \rho_{\overline{ZH}} \alpha_i \dot{\beta}_i + 2\Delta_{\alpha_i} E\dot{\alpha}_i - \Delta_H \varepsilon H \alpha_i \dot{\beta}_i \\ & - \Delta_Z \varepsilon Z \alpha_i \dot{\beta}_i) - 2[\Delta_H \varepsilon H \alpha_i v_i])hdV\end{aligned} \qquad (33)$$

where the entropy energy rate on the left is equal to a heat rate term, plus an energy term which defines the stress tensor at thermodynamic equilibrium as essentially the variation of internal energy with respect to the continuum strain tensor, plus an energy term which has accumulations from various energy contributions as a volume of $C_o \equiv mc_{oi}e_{ijk}a_jb_k$ of Zircaloy (essentially a volume of zirconium atoms containing a high density of hydrogen atoms [Duffin, 1988]) is chemically transformed and precipitated out as a zirconium hydride platelet, plus a transport of energy term as a flux of hydrogen atoms diffuse down spatial gradients in the chemical potential of hydrogen, and finally, plus a surface energy term which has accumulation from various contributions as existing hydride platelet change size along directions in the vector set ($\underline{a}$,$\underline{b}$,$\underline{c}$).

Several simplifications occurred in writing equation (33). One was setting to zero a term that contained the quasi-static equilibrium equation; that is,

$$\Delta_i \sigma_{ij} + f_j = 0 \qquad (34)$$

Also, the energy term $\Delta_H \varepsilon \dot{\bar{H}}$ was set to zero at points in R_o where hydride precipitation kinetics was not occurring because hydrogen atoms are conserved as interstitial atoms in solid solution with the Zircaloy at points other than where hydrogen atoms are chemically combined to form zirconium hydrides. Similarly, the energy term $\Delta_Z \varepsilon \dot{\bar{Z}}$ was set to zero at points in R_o where hydride precipitation kinetics was not occurring. The important results to note in equation

(33) are the two energy terms which have accumulations of various energy contributions for the precipitation and the size changes of platelets. These two energy terms have energy contributions from stress work, from the thermodynamic energetics of converting atoms of hydrogen ($\Delta_H\varepsilon$) and zirconium ($\Delta_Z\varepsilon$) to molecules of zirconium hydride ($\Delta_h\varepsilon$ per precipitated platelet and $\Delta_{\overline{ZH}}\varepsilon$ per molecule for size changes), and from surface energy along the boundary between the zirconium hydride and the Zircaloy. From these two energy terms, it is clear that stress work has the same directional influences on the energetics of precipitation and on the growth of hydride platelets in Zircaloy. In the following section, these terms are discussed in greater detail for the case of hydride platelets in a cylindrical Zircaloy spent fuel rod.

STRESS DEPENDENCE ON HYDRIDE KINETICS IN ZIRCALOY CLADDING

In the previous section, a thermodynamic model for various energetic terms that can change during precipitation of hydrides was developed. The resultant energy terms of the model are given in equation (33). For this model, equation (33) is a simple statement that entropy changes can occur from heat transport, stress-strain energy density changes, hydride precipitation kinetics, hydrogen transport, and hydride growth kinetics. For the following discussion, it is assumed that only adiabatic thermodynamic processes occur, thus the heat rate terms are set to zero. Then, it follows from classical thermodynamics [Gibbs, 1961; Onsager, 1931; deGroot, 1957] that the entropy change from the remaining energetic terms should not be negative. In addition and to simplify the thermodynamic discussion, it is assumed that the stress-strain energy density changes occur at thermodynamic equilibrium for all changes in $\Delta_i v_{j|}$; thus, the stress tensor is

$$\sigma_{ij} = (I_{mnij} - S_{mnij}) \Delta_{\gamma_{mn}}\varepsilon \qquad (35)$$

which defines the stress tensor in terms of the gradient of the internal energy with respect to the strain tensor $\gamma_{mn|}$; and is analogous to classical elasticity. For small $\gamma_{mn|}$ strains, the "S" tensor is small compared to the "I" tensor and linear elastic relationships are appropriate. Thus, in the following, it will be assumed that linear elasticity is adequate to describe the nominal stresses in thin-walled Zircaloy cladding. Note that this does not mean that the total Eulerian strain of equation (16) is small, because it also depends on the strain tensor $\gamma_{mn]}$ induced by hydride kinetics.

The above assumptions reduce equation (33) to hydride kinetics terms and a hydrogen transport term. In addition, the "stress" tensor denoted as σ^*_{ij} which is

$$\sigma^*_{ij} = \sigma_{ij} + S_{mnij}/\Delta_{\gamma_{mn}}|\varepsilon \tag{36a}$$

$$\doteq \sigma_{ij} \tag{36b}$$

after linearization because the "S" tensor has a higher order term in the strain tensor γ_{mn}|. Then equation (33) reduces to

$$\begin{aligned}\int_{R_o} \Delta_\eta \varepsilon \dot{\eta} dV = \int_{R_o} (&\sigma_{ij} C_{ij} - (\Delta_{\overline{ZH}} \varepsilon C * \rho_{\overline{ZH}} + 2\Delta_{\alpha_i} E\alpha_i \\ &- \Delta_H \varepsilon H C_o - \Delta_Z \varepsilon Z C_o)) \dot{\bar{h}} - \Delta_j (\Delta_H \varepsilon) v_j H \\ &+ (\sigma_{ij}(\dot{A}_{ij} + \dot{B}_{ij} + \dot{C}_{ij}) - (\Delta_{\overline{ZH}} \varepsilon \rho_{\overline{ZH}} \alpha_i \dot{\beta}_i + 2\Delta_{\alpha_i} E\dot{\alpha}_i \\ &- \Delta_H \varepsilon H \alpha_i \dot{\beta}_i) - \Delta_Z \varepsilon Z \dot{\beta}_i) - 2[\Delta_H \varepsilon H \alpha_i v_i]) h dV\end{aligned} \tag{37}$$

where the thermodynamic potential per hydride $\Delta_h\varepsilon$ has been replaced by substituting in the thermodynamic potential per zirconium hydride molecule as defined in equation (27). From equation (37), a general description of hydride kinetics in the context of irreversible thermodynamics couples the precipitation, the hydrogen transport, and the growth terms through Onsager "coefficients" (here coefficients would be generalized to operators). This means that from equation (37) there would be a total of five equations (eleven equations counting vector components) for the functions $\dot{\bar{h}}$, v_iH, $\dot{a}_i$, $\dot{b}_i$, and $\dot{m}$ which are coupled together by Onsager coefficients. The measures of thermodynamic nonequilibrium, which are the "thermodynamic forces", are the coefficient terms of the four rates and the hydrogen flux functions. A more complete discussion of equation (37) will be given in a future paper; here it is pointed out that the bias due to stress on the precipitation of hydrides and the bias due to stress on the growth of hydrides are functionally similar in the terms of equation (37). Therefore, only a discussion of hydride precipitation kinetics will be presented.

For these discussions, an equivalent physical assumption would be to consider hydride precipitation occurring rapidly such that no hydrogen transport or hydride growth has time to occur. Then, equation (37) has only the $\dot{\bar{h}}$ term, and the coefficient of $\dot{\bar{h}}$ is the nonequilibrium

thermodynamic "force" that causes the precipitation. In order to simplify the discussion for the case of hydrides in cylindrical Zircaloy cladding, consider only two possible species of hydride densities, radial hydride species h_r and tangential (hoop) hydride species h_θ where species are identified by the normal vector to the plane of the platelet. These species are illustrated in Figure 1, along with vector components that identify the effective dimensions of the two species q_r and q_θ as $(\underline{a}_r, \underline{b}_r, \underline{c}_r)$ and $(\underline{a}_\theta, \underline{b}_\theta, \underline{c}_\theta)$, respectively. The possibility of axial h_z hydride species is not discussed because the nominal σ_{zz} stress is approximately one-half the $\sigma_{\theta\theta}$ stress in the pressurized cladding and stress-dependent orientation of platelets from radial species h_r to tangential species h_θ occurs before any axial h_z species appear.

Using the notation illustrated in Figure 1, the internal energy change from the thermodynamic potentials in creating a h_r species of hydride platelet with $C^*_r \rho_{\overline{ZH}}$ molecules of zirconium hydride from $C_{or}Z$ and $C_{or}H$ atoms of zirconium and hydrogen is by definition

$$\Delta E_r(ZH_s \overleftarrow{\rightarrow} Z + sH) = (\Delta_Z \varepsilon ZC_{or} + \Delta_H \varepsilon HC_{or} - \Delta_{\overline{ZH}} \varepsilon \rho_{\overline{ZH}} C^*_r) \qquad (38a)$$

Similarly, the energy change for a h_θ species of hydride platelet is

$$\Delta E_\theta(ZH_s \overleftarrow{\rightarrow} Z + sH) = (\Delta_Z \varepsilon ZC_{o\theta} + \Delta_H \varepsilon HC_{o\theta} - \Delta_{\overline{ZH}} \varepsilon \rho_{\overline{ZH}} C^*_\theta) \qquad (38b)$$

Then, using equation (38) and the cylindrical notation, equation (33) reduces to a thermodynamic expression for entropy changes due to only the two species precipitation terms that is given by

$$\int_{R_o} \Delta_\eta \varepsilon \dot{\eta} dV = \int_{R_o} (\sigma_{rr}\, m\Delta c_{1r} e_{123} a_{2r} b_{3r} + \Delta E_r - 2\Delta_{\alpha_i} E_r \alpha_i)\, \dot{\bar{h}}_r + (\sigma_{\theta\theta}\, m\Delta c_{2\theta} e_{123} a_{3\theta} b_{1\theta} + \Delta E_\theta - 2\Delta_{\alpha_i} E_\theta \alpha_i)\, \dot{\bar{h}}_\theta dV \qquad (39)$$

With respect to hydride precipitation in Zircaloy cladding as the *temperature decreases* in a repository, the thermodynamic energy terms in equation (39) indicate that the independent creation of either h_r and h_θ species occurs whenever their corresponding coefficients (measures of thermodynamic nonequilibrium) are non-negative. Otherwise, entropy would decrease as hydrides formed which would contradict the classical statement of the Second Law of

Thermodynamics for adiabatic processes. In general, nonequilibrium thermodynamic precipitation equations for coupled hydride species interaction are

$$\dot{\bar{h}}_r = L_{rr} T_r + L_{r\theta} T_\theta \tag{40a}$$

$$\dot{\bar{h}}_\theta = L_{\theta r} T_r + L_{\theta\theta} T_\theta \tag{40b}$$

$$T_r = \sigma_{rr} m \Delta c_{1r} e_{123} a_{2r} b_{3r} + \Delta E_r - 2\Delta_{\alpha_i} E_r \alpha_i \tag{41a}$$

$$T_\theta = \sigma_{\theta\theta} m \Delta c_{2\theta} e_{123} a_{3\theta} b_{1\theta} + \Delta E_\theta - 2\Delta_{\alpha_i} E_\theta \alpha_i \tag{41b}$$

where T_r and T_θ are measures for thermodynamic nonequilibrium from equation (39) and (L_{rr}, $L_{r\theta}$, $L_{\theta r}$, $L_{\theta\theta}$) are positive-definite Onsager type "coefficients" to describe the precipitation kinetics of the hydride species, which in this case consists of various sizes of h_r and h_θ species. These Onsager "coefficients" are functional operators over the domain of hydride species. (Recall that growth of hydrides was negligible for this discussion.) Furthermore, from irreversible thermodynamics, the off-diagonal terms can be set equal and they need not be positive [deGroot, 1957]. For the case where the off-diagonal coefficients are set to zero and the diagonal coefficients are equal, then it follows from equation (40) that the probability for a h_r species versus a h_θ species is directly proportional to their associated thermodynamic forces, T_r versus T_θ, respectively. Therefore, the probability that an incipient platelet will precipitate as a h_r species remains large until the thermodynamic force T_θ is close to or exceeds T_r. After T_θ exceeds T_r, the probability that the incipient platelet precipitates as a h_θ platelet is larger. Furthermore, if the off-diagonal terms are negative in equation (40), then the probability of a h_r species versus a h_θ species decreases as T_θ increases given that T_r is essentially constant. Thus, for internally pressurized cladding, the probable hydride orientation depends on the state of stress as given in equations (40) and (41) through the thermodynamic forces for hydride precipitation. The experimental data indicate that at low internal pressures, the hydrides in cladding fabricated by roll forming techniques would have mainly radially oriented platelets [Ells, 1968]. However, reorientation can take place at higher stresses [Einziger and Kohli, 1984].

Placing this in context of spent fuel cladding stresses, the low pressurized cladding will have a low $\sigma_{\theta\theta}$ stress, and as the internal pressure of the cladding increases the $\sigma_{\theta\theta}$ stress component increases proportionally as the ratio of the clad's radius divided by the clad's wall-thickness (nominally it would be positive and an order of magnitude greater). The average σ_{rr} stress through the thickness of the clad will be of the same order as the internal pressure (nominally it would be negative and one-half of the internal pressure). Thus, an illustrative

plot of the two thermodynamic forces for the two hydride species versus internal cladding pressure would be as shown in Figure 2. This plot indicates that at low internal pressure, the radial thermodynamic force T_r is greater than the tangential thermodynamic force; however, as the internal pressure increases, $\sigma_{\theta\theta}$ increases and T_θ becomes greater than T_r. From this plot and equation (40), the expected rate, and consequently, the expected number of hydrides for each of the two species versus internal clad pressure would be as illustrated in Figure 3. At this time, no numbers for the densities of the species have been inferred from the literature, however, the literature indicates that around 100MPa (~ 15000 psi) hoop stress some reorientation of hydrides is expected to occur [Ells, 1968; Ells, 1970]. Clearly, the function dependence of this thermodynamic model (in terms of $\sigma_{\theta\theta}$ or internal pressure) would be consistent with the experimental data. Furthermore, the hydride data suggest that the thermodynamic energies for hydride precipitation, ΔE_r and ΔE_θ, are not equal in cladding fabricated by roll forming.

Finally, the thermodynamic model suggests a set of simple experiments to determine the stress dependence and values for the nonequilibrium thermodynamic forces of precipitation; namely, sections of spent fuel Zircaloy cladding with various internal pressures could be tested in a controlled decreasing temperature field. Furthermore, by controlling the rate at which the temperature field is decreased, possible influences of hydride growth and hydrogen transport on hydride precipitation kinetics could also be investigated.

SUMMARY

The influence of hydride precipitation on the Zircaloy cladding failure in a repository is primarily dependent on the orientation of the hydride platelets. Hydride platelets that precipitate with their normals in a radial direction are not expected to be an important factor in cladding failures. However, hydride platelets that precipitate with their normals in a tangential direction are expected to significantly increase the probability of cladding failures. This development of deformation and thermodynamic models that depend on hydride density (including orientation) have provided expressions to calculate the probable strain field induced by hydrides and the functional dependence for probable hydride orientation on the state of nominal stress in the cladding. These deformation and thermodynamic models for hydride kinetics extend those that currently exist in the literature [Ells, 1970]. These models provide a basis for planning and analyzing future experiments to describe Zircaloy cladding failure due to hydride precipitation. A description of the probable failure rate due to hydrides in Zircaloy

cladding is a necessary and important part of representing the amount of UO_2 spent fuel that may be exposed to oxidation and dissolution processes in a proposed nuclear waste repository.

REFERENCES

Boltzmann, Ludwig (1964) Lectures on Gas Theory, Translated by S. G. Brush, University of California Press, Berkeley, CA.

Christian, J. W. (1965) Phase Transformations, in Physical Metallurgy, edited by R. W. Cahn, North-Holland Pub. Co., Chapter 10, pp 443.

deGroot, S. R. (1957) Thermodynamics of Irreversible Processes, North Holland Pub. Co., Amsterdam.

Duffin, W. (1988) Personal discussion on hydride precipitation sites and local inhomogeneous hydrogen trapping in Zircaloy.

Einziger, R. E., and R. Kohli (1984) Low-Temperature Rupture Behavior of Zircaloy-Clad Pressurized Water Reactor Spent Fuel Rods under Dry Storage Conditions, Nuc. Tech., Vol. 67, pp 107.

Ells, C. E. (1968) Hydride Precipitates in Zirconium Alloys, J. Nuc. Mat., Vol. 28. pp 129.

Ells, C. E. (1970) The Stress Orientation of Hydride in Zirconium Alloys, J. Nuc. Mats., Vol. 34, pp 306.

Eringen, A. C. (1967) Mechanics of Continua, John Wiley Pub., NY.

Gibbs, J. (1961) The Scientific Papers of J. Willard Gibbs, Vol. 1, Dover Pub. Inc., NY.

Hardy, H. K., and T. J. Heal (1961) Report on Precipitation, in Progress in Metal Physics, Vol. 5, pp 143, 2nd Printing Pergamon Press.

Leger, M., and A. Donner (1984) The Effect of Stress on Orientation of Hydrides in Zirconium Alloy Pressure Tube Materials, Canadian Meta. Qu., Vol. 24, pp 235.

Lupis, C.H.P. (1983) Chemical Thermodynamics of Materials, Elsevier Science Publish., NY.

Onsager, L. (1931) Reciprocal Relations in Irreversible Processes; I and II., Physics Rev., Vol. 37 and 38, pp 405 and pp 2265.

Ostberg, G. (1968) Crack Propagation in Hydrided Zircaloy-2, Int. J. Fract. Mech., Vol. 4, pp 95.

Sawatzky, A. (1960) J. Nucl. Mat., Vol. 2, pp 321.

Stout, R. B. (1981) Modelling the Deformations and Thermodynamics for Materials Involving a Dislocation Kinetics, Cryst. Latt. Def., Vol. 9, pp 65.

Stout, R. B. (1984) Deformation and Thermodynamic Response for a Crack Dislocation Model of Brittle Fracture, Eng. Fract. Mech., Vol. 19, pp 545.

Stout, R. B. (1986) On Kinematic and Thermodynamic Conditions for Mass, Dislocation, Momentum, and Energy Densities Across a Propagating Surface of Discontinuity, Cryst. Latt. Def. and Amorph. Mat., Vol. 11, pp 329.

Stout, R. B. (1989) Statistical Model for Particle-Void Deformation Kinetics in Granular Materials During Shock Wave Propagation, Lawrence Livermore National Laboratory, Report UCRL-101623, July.

ACKNOWLEDGMENTS

The author wishes to first thank Lydia Grabowski and Bonnie Pitrowski for excellent organization and most timely typing of this paper. In addition, the author wishes to acknowledge the many immensely helpful discussions with Dr. Walter Duffin, of Westinghouse Corp., Pittsburgh, PA, who has freely provided his profound physical insight into many mechanistic aspects of hydrogen and hydrides in Zircaloy. Also, the author wishes to thank Dr. Homer Weed for the gracious and patient sharing of his vast practical and theoretical knowledge of chemical thermodynamics.

Work performed under the auspices of the U.S. Department of Energy, Office of Civilian Radioactive Waste Management, Yucca Mountain Project Office, by the Lawrence Livermore National Laboratory under contract W-7405-ENG-48.

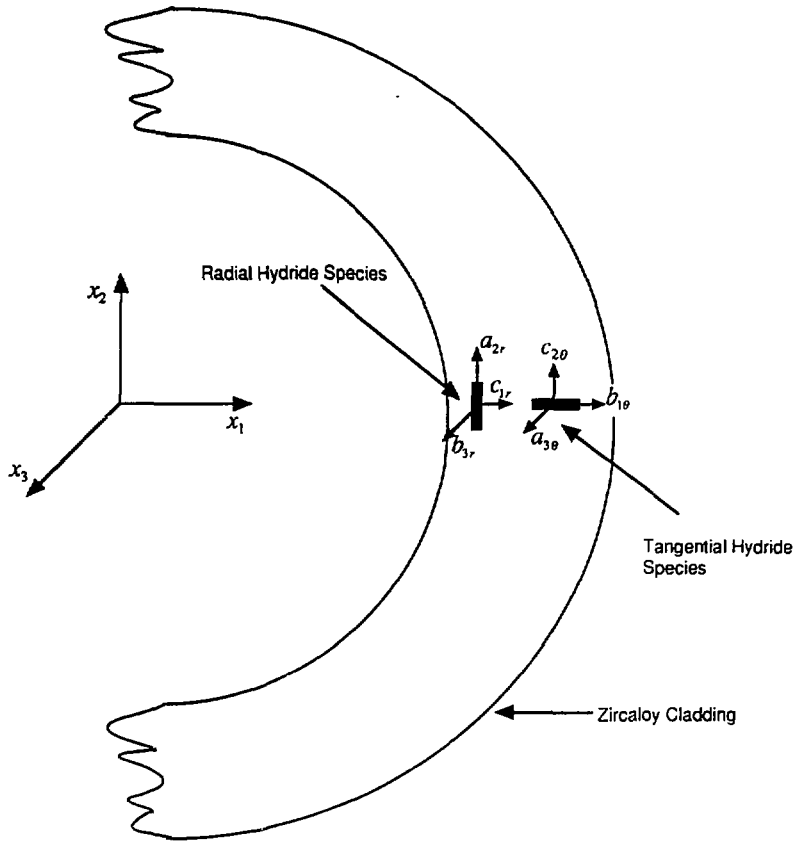

Figure 1. Illustration of a radial hydride species (a_{2r}, b_{3r}, c_{1r}) and a tangential hydride species ($a_{3\theta}$, $b_{1\theta}$, $c_{2\theta}$) in a section of Zircaloy cladding.

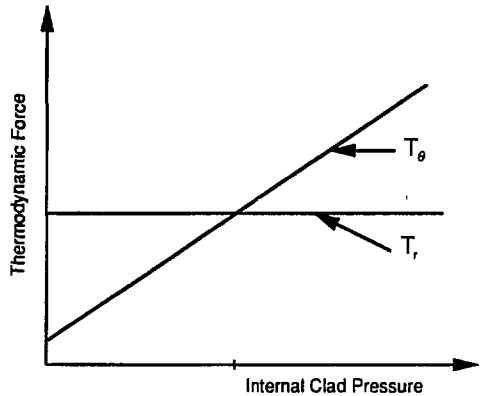

Figure 2. Illustration of the nonequilibrium thermodynamic forces for hydride precipitation, T_r and T_θ, versus internal clad pressure (induced stress dependence in clad).

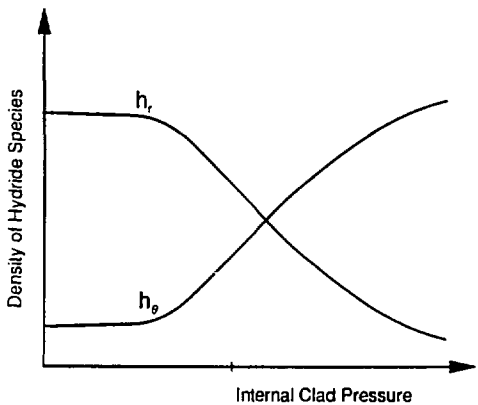

Figure 3. Illustration of hydride precipitation densities for h_r and h_θ species versus "stress" dependence induced by internal clad pressure.